New Journal of Physics
The open access journal at the forefront of physics

Deutsche Physikalische Gesellschaft DPG
IOP Institute of Physics

Published in partnership with: Deutsche Physikalische Gesellschaft and the Institute of Physics

OPEN ACCESS

RECEIVED
2 August 2021

ACCEPTED FOR PUBLICATION
9 September 2021

PUBLISHED
27 September 2021

PAPER

Single-ion induced surface modifications on hydrogen-covered Si(001) surfaces—significant difference between slow highly charged and swift heavy ions

C Länger[1], P Ernst[2], M Bender[3], D Severin[3], C Trautmann[3,4], M Schleberger[2] and M Dürr[1,*]

[1] Institut für Angewandte Physik and Zentrum für Materialwissenschaften, Justus-Liebig-Universität Giessen, 35392 Giessen, Germany
[2] Fakultät für Physik and CENIDE, Universität Duisburg-Essen, 47057 Duisburg, Germany
[3] GSI Helmholtzzentrum für Schwerionenforschung, 64291 Darmstadt, Germany
[4] Fachbereich Materialwissenschaften, Technische Universität Darmstadt, 64287 Darmstadt, Germany
[*] Author to whom any correspondence should be addressed.

E-mail: michael.duerr@ap.physik.uni-giessen.de

Keywords: swift heavy ions, silicon, highly charged ions, scanning tunneling microscopy, STM

Supplementary material for this article is available online

Abstract

Hydrogen-covered Si(001) surfaces were exposed to swift heavy ions (SHI) and slow highly charged ions (HCI). Using scanning tunneling microscopy as analysis tool, the ion-induced modifications on the surface were resolved on the atomic scale. SHI were found occasionally to lead to changes which are restricted to one or two Si surface atoms. In comparison, HCI form pits of several nanometers in diameter, depending on the potential energy of the HCI. These observations are in contrast to many material systems for which similar effects of SHI and HCI have been observed. The results suggest a high stopping power threshold for SHI-induced modifications in crystalline silicon with major implications for the application in silicon-based nanotechnology.

1. Introduction

The formation of nanostructures on the surface of solids by either swift heavy ions (SHI) or slow highly charged ions (HCI) has been observed for many different materials, including oxides, halides, polymers, and 2D materials [1–3]. Both ion types interact primarily with the electronic subsystem of the target material; it has therefore been suggested that the subsequent relaxation mechanisms might be similar and, as a consequence, should lead to similar modifications. The evident morphological similarity of SHI- and HCI-induced nanostructures does indeed support this assumption. In addition, the two-temperature model (TTM) [4], which has been applied to interpret SHI related data with great success [5–8], has recently also been applied to explain data from HCI irradiations [9–12].

The TTM takes into account that the ion projectiles deposit their energy in the electronic subsystem and, via electron–phonon coupling, produce a thermal spike in the atomic system. Depending on the energy density and the material properties, the thermal spike can be sufficient to drive phase transitions such as melting. The relevant phonons are generated on the timescale of picoseconds, while the initial electronic excitation happens within femtoseconds and forms a highly localized non-equilibrium state. The details of the coupling of these two subsystems are known to be strongly influenced by material properties (e.g. conductive versus insulating, crystalline versus amorphous structure). Track formation in the bulk and damage creation on the surface are thus both linked to a stopping power threshold which depends on the materials investigated [1].

A most interesting test case for the comparison of SHI and HCI is crystalline silicon, for which no track formation was observed in the case of irradiation with monoatomic SHI up to a stopping power of

21 keV nm^{-1} [13, 14]. Only when using C_{60} cluster ions (total kinetic energy of 30–40 MeV) [15, 16] with increased stopping power and effective energy density due to the lower ion velocity, ion tracks in the bulk of crystalline silicon have been observed and a stopping power threshold of ≈30 keV nm^{-1} was deduced. On the other hand, HCI irradiation of Si(111) 7 × 7 was shown to induce damage in areas of several nanometers in diameter with a clear dependence on the potential energy of the employed ions [17–19].

The unusually high stopping power threshold was not reproduced in TTM calculations, which predict a threshold between 5 and 10 keV nm^{-1} for ion track formation in Si [14, 20, 21]. Possible reasons for this discrepancy might be found in the details of the energy transfer from the electronic to the atomic subsystem, e.g. the temporal and spatial distribution of low energy electrons [22], resulting in a lower electron–phonon-coupling in silicon than assumed in the calculations. It has also been speculated that this seemingly high threshold is not caused by the details of the excitation process as such but that fast recrystallization of the silicon lattice suppresses the formation of permanent damage or renders it at least too small (or too short-lived) to be imaged correctly by the *ex situ* analysis tools applied. As an example, the different response of various oxides to swift Xe ions have been discussed in this way [23].

For the further interpretation of ion-induced phenomena in silicon, it is thus of great importance to rule out recrystallization as the origin for the high stopping power threshold. In our experiments, we made use of hydrogen passivated Si(001) surfaces in combination with scanning tunneling microscopy (STM) in order to explicitly address this point: on one hand, hydrogen desorption from these surfaces leads to distinct signatures in STM measurements [24, 25] that can be resolved on the atomic scale. On the other hand, desorption of hydrogen under ultra-high vacuum (UHV) conditions is an irreversible process. Thus, if a thermal spike would lead to hydrogen desorption at the surface at any time after ion impact, this modification would be observable even if the substrate itself recrystallizes during the further process. With a resolution on the atomic scale, the experiments are sensitive to very small changes on the surface. Furthermore, working under UHV conditions excludes the formation of silicon oxide on the surface, which easily forms ion-induced volume tracks and surface hillocks [26].

For the irradiation, we used U ions of highest energy deposition available with monoatomic ions (4.8 MeV/u, 1.14 GeV, dE/dx = 27 keV nm^{-1}). Even for those extreme conditions, we observed, if at all, only a very small effect of SHI on the H/Si(001) surface; the detected signatures were restricted to one or two silicon surface atoms. We compare our results for SHI on H/Si(001) with the effect of HCI (Xe^{40+} and Xe^{45+}) carrying a maximum potential energy of E_{pot} ≈ 60 keV (Xe^{45+}) and a kinetic energy of 225 keV. For HCI, we found substantial disorder and removal of material on/from the H/Si(001) surface caused by single ion impacts, comparable to results on clean Si(111). We discuss our results in terms of a high stopping power threshold for SHI-induced modifications in silicon.

2. Experimental

Surface microscopy investigations were performed at Justus Liebig University Giessen with a variable temperature STM (Omicron VT-STM) mounted in a UHV chamber with a base pressure $<1 \times 10^{-10}$ mbar. The STM measurements were performed in constant-current-mode using a tungsten tip and a sample bias of $U_t = -2$ V; the tip thus images surfaces of constant density of states at the given energy, i.e. filled electronic surface states in case of negative sample bias. Si(001) samples were prepared by degassing at 700 K and repeated direct current heating cycles to above 1450 K; cooling rates of about 1 K s^{-1} led to a well-ordered 2 × 1 reconstruction [27, 28]. Hydrogen terminated surfaces were prepared by exposing a heated Si(001) surface ($T_s \simeq 650$ K) to atomic hydrogen, leading to either a 2 × 1 or 3 × 1 H/Si(001) reconstruction, depending on the exact surface temperature. Atomic hydrogen was generated by dissociation of molecular hydrogen at a hot tungsten filament ($T_F \simeq 2000$ K).

Figure 1 (top) shows filled state STM images of both, the H/Si(001) 2 × 1 and 3 × 1 reconstruction, as well as a ball-and-stick model of the respective reconstruction. In the bottom, a schematic representation of the performed irradiation experiments is shown. The samples which were prepared in the STM apparatus were transported under UHV to the respective ion beam facility. Irradiation with SHI was realized at UNILAC of GSI Helmholtzzentrum für Schwerionenforschung; beam parameters were: $^{238}U^{28+}$ with $E_{kin} = 1.14$ GeV (4.8 MeV/u) at three different fluences of 0.2, 1.8, and 5×10^{11} cm^{-2}. Irradiation with HCI was performed at University Duisburg-Essen at the HICS beamline [29] equipped with a commercial DREEBIT EBIS-A ion source; beam parameters were: $^{129}Xe^{40+}$ with $E_{pot} = 38.5$ keV at a fluence of ≈3×10^{11} cm^{-2} as well as $^{129}Xe^{45+}$ with $E_{pot} = 58.8$ keV at a fluence of ≈1×10^{11} cm^{-2}. Kinetic energy was $E_{kin} = 225$ keV in both cases. Both, SHI and HCI irradiation, were performed with the ion beam perpendicular to the surface. After irradiation, the samples were transferred back to the STM chamber, again without breaking the vacuum using a UHV transport system with mobile pumping unit (base

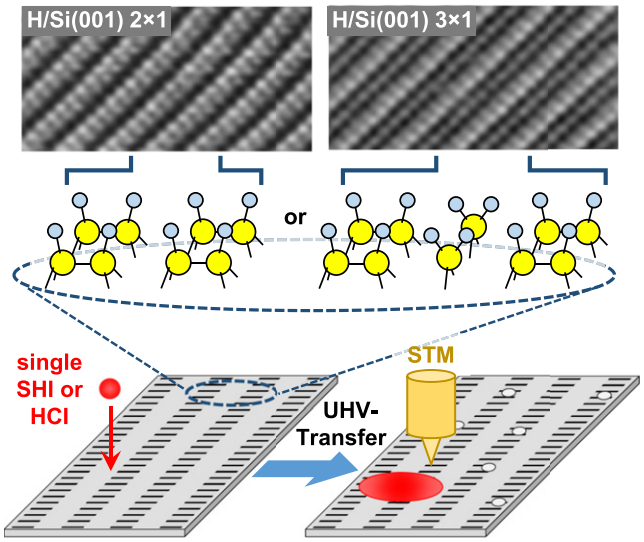

Figure 1. Top: filled state STM images (5×10 nm^2; $U_t = -2$ V; $I_t = 0.5$ nA) of hydrogen-covered Si(001) surfaces with 2×1 (left) and 3×1 (right) reconstruction. Center: ball-and-stick models of the respective surface reconstructions (blue balls: hydrogen atoms; yellow balls: silicon atoms). Bottom: schematic representation of the experiments: after preparation of the H/Si(001) surfaces and sample transfer in UHV to the respective ion sources, the samples were irradiated with SHI or HCI (the red arrow indicates the impact of an individual ion). After UHV transfer back to the analysis chamber, defects on the surface (indicated by the white and red signatures) were investigated by means of STM.

pressure $<1 \times 10^{-10}$ mbar). In the load locks of the respective chambers, the samples were briefly exposed to a residual gas pressure $<1 \times 10^{-9}$ mbar. Alle experiments were performed at room temperature.

3. Results

In figure 2, STM images ($U_t = -2$ V; $I_t = 0.5$ nA) of an H/Si(001) surface before and after irradiation with $^{238}U^{28+}$ ions are shown. In all images, both before and after irradiation, the dimer row reconstruction of Si(001) is clearly observed. The unirradiated samples exhibit a few additional bright and dark features (figure 2(a)). The dark features are typically ascribed to missing dimer defects. The bright features are assigned to silicon surface atoms which are not saturated by a hydrogen atom [24, 25]. The respective dangling bond states show a higher density of states at the chosen sample bias leading to the increased brightness in the images. In principle, additional adsorbates on the H/Si(001) surface can lead to such bright features as well; however, in the case of the freshly prepared surfaces, we can largely exclude such contaminations.

STM images after irradiation with the lowest fluence (0.2×10^{11} cm^{-2} which equals 0.4 single ion impacts on the depicted area) and highest fluence (5×10^{11} cm^{-2} equaling nine single ion impacts on the depicted area) applied in our experiments are shown in figures 2(b) and (c), respectively. After irradiation, the well-defined surface reconstruction was still intact. However, more bright features were observed than prior to irradiation whereas the number of dark features stays approximately the same. The number of the additional bright features is increasing with increasing fluence, however, the observed density is significantly higher than the applied fluence (approx. 5 to 10 times, compare figure S1 (https://stacks.iop.org//NJP/23/093037/mmedia) in the supporting information). Reference samples kept in the irradiation chamber but positioned outside the ion beam did not show these additional features. Therefore the results for the irradiated samples indicate ion-induced effects which were either directly or indirectly induced by SHI.

We analyzed the spatial distribution of the bright features by evaluating the distribution of next neighbor distances in the STM images; for comparison, Monte-Carlo simulations of a purely statistical distribution were performed (figure S2 in the supporting information). The experimental results and the simulations are almost identical (figure S2) pointing toward a purely stochastic distribution of bright features after irradiation.

The experimental results can thus be summarized as follows: (i) we observe additional bright spots, but with a higher density (5–10 times) than expected from the applied fluence when assuming that every ion impact leads to one single bright feature. No additional dark features were observed. (ii) The bright features do not show any spatial accumulation on the surface but follow a stochastic distribution. From the latter observation, we can exclude that a single ion impact leads to several of the bright features, as they then

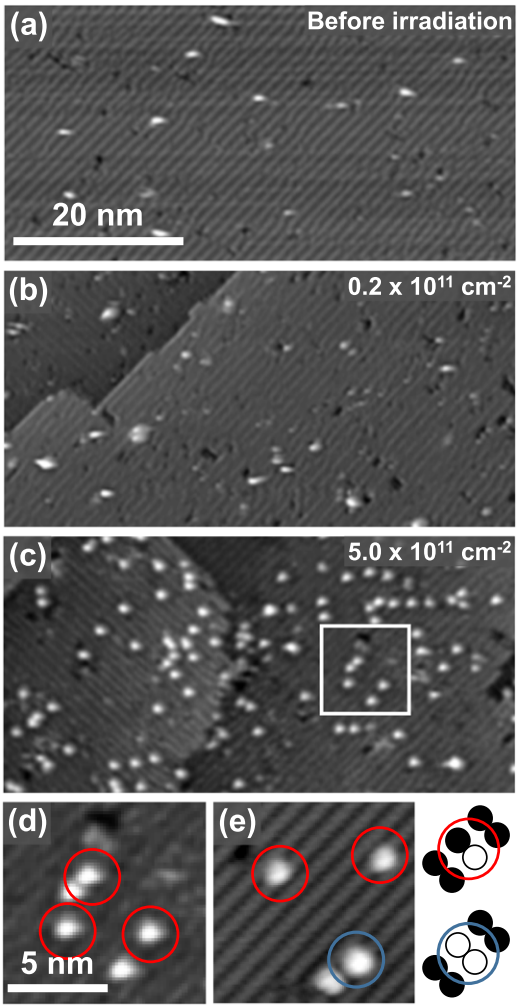

Figure 2. Filled state STM images ($U_t = -2$ V; $I_t = 0.5$ nA) of hydrogen-terminated Si(001) surfaces before and after irradiation with $^{238}U^{28+}$ ions at different fluences. (a) Before irradiation, the H/Si(001) surface shows a mixture of 3×1 and 2×1 reconstruction with few dark and bright features. (b) H/Si(001) surface after irradiation with the lowest ion fluence used in the experiments (0.2×10^{11} cm^{-2} equaling 0.4 single ion impacts on the depicted area). The surface reconstruction is preserved. (c) For the highest fluence (5.0×10^{11} cm^{-2} equaling nine single ion impacts on the depicted area), a distinct increase of bright features is observed after irradiation. (d) A blow up of (c) indicates the size of the bright features. (e) H/Si(001) after thermal desorption of a small amount of hydrogen [24, 30]; the observed features are of similar size as in (d).

should be accumulated around the impact point: with the known mobility of hydrogen on silicon and its temperature dependence [25], a complete equilibration of an initially inhomogeneous distribution is not possible on the relevant time scales. The majority of the bright features may thus be attributed to contaminations adsorbed on the surface. They could result, e.g. from ion-induced sputtering in the vicinity of the sample, e.g. from the ceramic sample holder plate. Indeed, when scanning the surface with the STM tip, some of the bright features could be moved on the surface. This is not possible for covalently bound hydrogen at the tunneling parameters employed.

Still, some of the bright features might directly origin from a single ion impact and ion-induced hydrogen desorption. It is thus interesting to compare the size of the bright features with images of a hydrogen terminated Si(001) surface on which isolated dangling bonds and dangling bond pairs were created intentionally by means of thermal hydrogen desorption and diffusion as shown in figure 2(e) [24]. This comparison clearly indicates that the bright features on the irradiated surfaces, as shown in figures 2(c) and (d), are restricted to one or two silicon surface atoms. We thus conclude that the single ion impacts do not lead to surface modifications larger than one silicon dimer. Moreover, as the hydrogen-terminated surface stays intact across the entire irradiated area, we exclude that the impact of a single ion leads to local melting followed by perfect recrystallization. Hydrogen desorption occurs at a much lower surface temperature than surface melting or ablation [30]; under UHV conditions, hydrogen desorption is irreversible as the hydrogen partial pressure is low and hydrogen dissociation on silicon shows a very low reactivity [24, 31]. Thus, even if the surface recrystallized after temporal melting (thermal spike), the originally adsorbed hydrogen would be desorbed. In consequence, the molten/recrystallized areas would

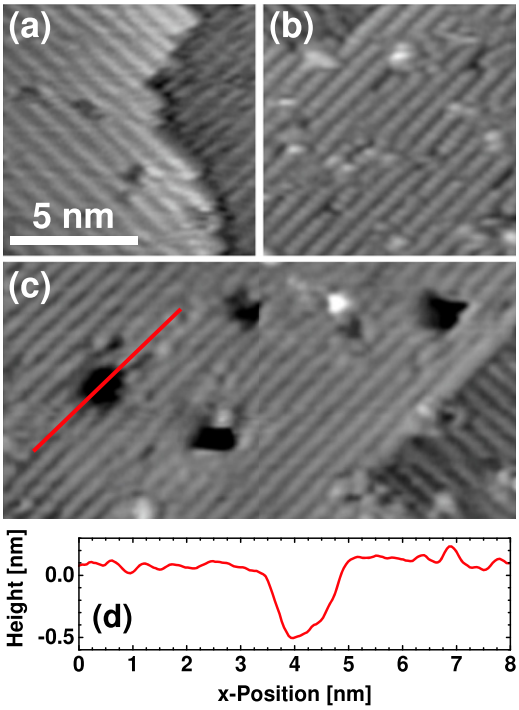

Figure 3. Filled state STM images ($U_t = -2$ V; $I_t = 0.5$ nA) of a hydrogen-terminated Si(001) surface before and after irradiation with $^{129}Xe^{45+}$ ions ($E_{pot} = 58.8$ keV; $E_{kin} = 225$ keV). (a) Before irradiation, the H/Si(001) surface shows very few small dark spots. After the irradiation, a slight increase of small dark and bright features is observed in areas outside (b) and inside (c) the ion beam spot on the sample. On the irradiated area of the sample (c), well-defined holes of about 2.3 ± 0.3 nm in diameter are observed. (d) Height profile through one impact area as indicated by the red line in (c).

show up in the STM images with higher brightness since the clean silicon dimers (without hydrogen adsorbed) appear brighter due to a higher density of states probed by the STM at the given tunneling bias.

In the following, we investigate how the results obtained with SHI compare with HCI irradiation of the H/Si(001) surface. Figure 3 shows filled state STM images ($U_t = -2$ V; $I_t = 0.5$ nA) of a hydrogen-terminated Si(001) 2×1 surface before and after irradiation with $^{129}Xe^{45+}$ ions ($E_{pot} = 58.8$ keV; $E_{kin} = 225$ keV). Before irradiation, the H/Si(001) surface exhibits a few small dark spots, which correspond to defects originating from sample preparation (figure 3(a)). Some bright features as present in figure 2(a) were also observed on larger scale images. After irradiation with $^{129}Xe^{45+}$ ions, well-defined pits of in average 2.3 ± 0.3 nm in diameter appear in the irradiated area of the sample (figure 3(c) and figure S3 in the supporting information). Within the error bars of the applied fluence, the number density of the pits (0.5×10^{11} cm^{-2}) agrees well with the number of ion impacts per surface area. The red line in figure 3(c) indicates a line scan through the impact area, the corresponding height profile is shown in figure 3(d). The apparent depth of this pit is ≈ 0.5 nm, i.e. several atomic layers in depth. Due to the limitations of measuring depth profiles with high aspect ratio by means of STM, this value can be seen as a lower limit. After the irradiation, a slight increase of small dark and bright features is also observed; they are assigned to the UHV transfer and sample handling procedure before and after the irradiation (compare figure 3(b)).

Irradiation of H/Si(001) with $^{129}Xe^{40+}$ ions ($E_{pot} = 38.5$ keV) also leads to clear signatures of ion-induced damage on the surface (figures S3 and S4). However, in contrast to the effect of the $^{129}Xe^{45+}$ ions, the observed pits are less well defined in shape and less deep (≈ 0.2 nm). Some accumulation of disordered material is observed at the rim of the pits and the pits are smaller than after irradiation with Xe^{45+} ions (figure S5). Within the error bars, the number density of observed pits (2×10^{11} cm^{-2}) also agrees well with the applied fluence.

4. Discussion

The presented results for SHI experiments on crystalline silicon substrates differ qualitatively from the results of SHI on various insulator materials [1, 32] or compound semiconductors [13, 33]. In both material classes, SHI irradiation leads to the formation of permanent nanostructures. Except for the STM experiments by Osmani *et al* on the impact of xenon ions on Si(111) ($E_{kin} = 0.12$ GeV; $dE/dx = 12$ keV nm^{-1}) [14], only very few experiments were reported for crystalline silicon so far. No

structural change induced by the impact of SHI was resolved in this former study, even when irradiating under glancing angle of incidence ($< 2°$ with respect to the surface) resulting in a higher energy deposition close to the surface.

From the observation of the intact hydrogen-covered Si(001) surface after irradiation with SHI, track formation followed by complete reconstruction/recrystallization is largely ruled out; from our STM analysis we can exclude surface modifications larger than a few surface atoms in size. The stopping power of the uranium ions applied in this study was 27 keV nm^{-1} (figure S6), the results thus suggest a threshold above 27 keV nm^{-1}, higher than the value predicted so far from the thermal spike model [14].

Furthermore, the results obtained with SHI on hydrogen-covered silicon clearly differ from the results of our experiments with HCI on H/Si(001). The latter show permanent crater-like damage structures of 1–3 nm in diameter; the observed pit size is larger for ions with higher energy. These results are comparable to the results of experiments with highly charged iodine ions (q between 30 and 50) on Si(111) 7×7 [17–19] which produced surface damage with radii between 1 and 3 nm, as well.

At this point, we would like to note that with $E_{kin} = 225$ keV, the Xe ions employed in our experiment are close to the maximum of the contribution of nuclear stopping to the total stopping power (figure S7). However, the absolute value is low (2 keV nm^{-1} in equilibrium charge state) when compared to the total potential energy available from the $^{129}Xe^{40+}$ and $^{129}Xe^{45+}$ ions. This goes along with the clear increase of the induced damage with the potential energy of the impacting ions when keeping the kinetic energy constant, which also points toward a major influence of E_{pot} for the formation of the observed damage.

So how can we explain the apparent difference between the impact of the SHI and HCI on crystalline silicon? In earlier experiments with 30 and 40 MeV C_{60} ions of $\approx$ 50 keV nm^{-1} electronic stopping power, track formation in Si was evidenced. From extrapolation of these data, a threshold of $\approx$ 30 keV nm^{-1} was predicted [15, 16]. With 27 keV nm^{-1}, we are just below this predicted threshold. In principle, the surface should exhibit a somewhat lower threshold for mainly two reasons: (i) the broken bonds at the surface reduce the effective binding energy (ii) it will reflect and thus increase the effective heat flux (although this might be of minor importance for perpendicular incidence). Regarding C_{60} projectiles compared to our U ions, one has to consider the following difference: the much lower velocity of 30 or 40 MeV C_{60} clusters leads to a higher energy density than in the case of the 1.14 GeV U ions. At high velocities, the energy is spread into a larger volume and thus the required critical stopping power is expected to increase [34].

Regarding the effective energy deposition of SHI and HCI, it has to be considered that the electrons generated by SHI are typically high in energy and leave the impact area rather fast [22, 35], thus lowering the effective energy density. Furthermore, the strength of electron–phonon coupling depends on the energy distribution of the excited electrons and thus on their thermalization. In contrast, the impact of an HCI is associated with the creation of many electrons of rather low energies [36] confining the energy closer to the impact point. It is these electrons which effectively transfer the energy to the lattice by creating phonons [20, 35].

The energy effectively deposited is usually estimated to be between 50% and 80% [10, 37, 38]. Taking additionally into account that the energy of the HCI is deposited within a depth of 1 nm (as a conservative estimate [9]), an energy per track length of 30–46 keV nm^{-1} is derived for Xe^{45+} ions. For Xe^{40+} ions with an energy per track length of about 20–30 keV nm^{-1}, the HCI-induced damage features are substantially smaller. With a less efficient energy deposition in the case of SHI, it seems reasonable to expect a stopping power threshold $\geqslant$ 30 keV nm^{-1}. Our data thus rule out the occurrence of a thermal spike in Si which is high enough to induce track formation and surface damage structures with monatomic SHI. We attribute this to a high stopping power threshold due to inefficient energy deposition in crystalline silicon [22].

5. Conclusion

In conclusion, we observed significant differences in the interaction of SHI and HCI with a crystalline hydrogen-covered Si(001) surface. For SHI with a stopping power of 27 keV nm^{-1}, the upper limit for single-ion induced surface damage was determined to be in order of 1–2 silicon atoms in size. In contrast, the impact of single HCI with a potential energy between 40 and 60 keV results in surface pits of 1–3 nm in diameter. As we could exclude recrystallization of silicon after SHI impacts, the striking difference between the effect of HCI and SHI was attributed to a high stopping power threshold operative in the case of SHI. This high threshold could result from fast spatial energy redistribution in combination with low electron phonon coupling for the electrons excited in crystalline silicon by swift heavy ion impact. The U ions we employed in our experiments exhibit the highest stopping power which can be realized in silicon with monoatomic SHI. Our results thus suggest that nanoscale materials' processing based on the impact of single monoatomic ions cannot be applied to crystalline silicon.

Acknowledgment

We acknowledge financial support by HICforFAIR, HGSHire (CL), DFG through CRC 1242 (Project ID 278162697), and BMBF (Projects 05K19RG1 and 05K16PG2). The results presented here are based on a UMAT experiment, which was performed at the M-branch of the UNILAC at the GSI Helmholtzzentrum für Schwerionenforschung, Darmstadt (Germany) in the framework of FAIR Phase-0.

Data availability statement

The data that support the findings of this study are available upon reasonable request from the authors.

ORCID iDs

C Trautmann https://orcid.org/0000-0001-7058-6340
M Schleberger https://orcid.org/0000-0002-5785-1186
M Dürr https://orcid.org/0000-0002-4676-8715

References

[1] Aumayr F, Facsko S, El-Said A S, Trautmann C and Schleberger M 2011 Single ion induced surface nanostructures: a comparison between slow highly charged and swift heavy ions *J. Phys.: Condens. Matter.* **23** 393001
[2] Li Z and Chen F 2017 Ion beam modification of two-dimensional materials: characterization, properties, and applications *Appl. Phys. Rev.* **4** 011103
[3] Schleberger M and Kotakoski J 2018 2D material science: defect engineering by particle irradiation *Materials* **11** 1885
[4] Toulemonde M, Dufour C and Paumier E 1992 Transient thermal process after a high-energy heavy-ion irradiation of amorphous metals and semiconductors *Phys. Rev.* B **46** 14362
[5] Toulemonde M, Paumier E and Dufour C 1993 Thermal spike model in the electronic stopping power regime *Radiat. Eff. Defects Solids* **126** 201
[6] Toulemonde M, Dufour C, Meftah A and Paumier E 2000 Transient thermal processes in heavy ion irradiation of crystalline inorganic insulators *Nucl. Instrum. Methods Phys. Res.* B **166–167** 903
[7] Daraszewicz S L and Duffy D M 2011 Extending the inelastic thermal spike model for semiconductors and insulators *Nucl. Instrum. Methods Phys. Res.* B **269** 1646
[8] Lang M, Devanathan R, Toulemonde M and Trautmann C 2015 Advances in understanding of swift heavy-ion tracks in complex ceramics *Curr. Opin. Solid State Mater. Sci.* **19** 39
[9] El-Said A S *et al* 2008 Creation of nanohillocks on CaF_2 surfaces by single slow highly charged ions *Phys. Rev. Lett.* **100** 237601
[10] Karlusic M and Jaksic M 2012 Thermal spike analysis of highly charged ion tracks *Nucl. Instrum. Methods Phys. Res.* B **280** 103
[11] Dufour C, Khomrenkov V, Wang Y Y, Wang Z G, Aumayr F and Toulemonde M 2017 An attempt to apply the inelastic thermal spike model to surface modifications of CaF_2 induced by highly charged ions: comparison to swift heavy ions effects and extension to some others material *J. Phys.: Condens. Matter.* **29** 095001
[12] Kozubek R, Ernst P, Herbig C, Michely T and Schleberger M 2018 Fabrication of defective single layers of hexagonal boron nitride on various supports for potential applications in catalysis and DNA sequencing *ACS Appl. Nano Mater.* **1** 3765
[13] Kamarou A, Wesch W, Wendler E, Undisz A and Rettenmayr M 2008 Radiation damage formation in InP, InSb, GaAs, GaP, Ge, and Si due to fast ions *Phys. Rev.* B **78** 054111
[14] Osmani O *et al* 2012 Damage in crystalline silicon by swift heavy ion irradiation *Nucl. Instrum. Methods Phys. Res.* B **282** 43
[15] Canut B, Bonardi N, Ramos S M M and Della-Negra S 1998 Latent tracks formation in silicon single crystals irradiated with fullerenes in the electronic regime *Nucl. Instrum. Methods Phys. Res.* B **146** 296
[16] Dunlop A, Jaskierowicz G and Della-Negra S 1998 Latent track formation in silicon irradiated by 30 MeV fullerenes *Nucl. Instrum. Methods Phys. Res.* B **146** 302
[17] Tona M *et al* 2007 Nano-crater formation on a Si(111)-(7 × 7) surface by slow highly charged ion-impact *Surf. Sci.* **601** 723
[18] Tona M *et al* 2007 Nanofabrication on a Si surface by slow highly charged ion impact *Nucl. Instrum. Methods Phys. Res.* B **256** 543
[19] Tona M, Watanabe H, Takahashi S, Nakamura N, Yoshiyasu N, Sakurai M, Yamada C and Ohtani S 2007 Potential sputtering from a Si surface by very highly charged ion impact *Nucl. Instrum. Methods Phys. Res.* B **258** 163
[20] Murat M, Akkerman A and Barak J 2011 Can swift heavy ions create latent tracks in silicon? *Nucl. Instrum. Methods Phys. Res.* B **269** 2649
[21] Khara G S, Murphy S T, Daraszewicz S L and Duffy D M 2016 The influence of the electronic specific heat on swift heavy ion irradiation simulations of silicon *J. Phys.: Condens. Matter.* **28** 395201
[22] Medvedev N A, Rymzhanov R A and Volkov A E 2015 Time-resolved electron kinetics in swift heavy ion irradiated solids *J. Phys. D: Appl. Phys.* **48** 355303
[23] Rymzhanov R A, Medvedev N, O'Connell J H, Janse van Vuuren A, Skuratov V A and Volkov A E 2019 Recrystallization as the governing mechanism of ion track formation *Sci. Rep.* **9** 3837
[24] Dürr M and Höfer U 2006 Dissociative adsorption of molecular hydrogen on silicon surfaces *Surf. Sci. Rep.* **61** 465
[25] Dürr M and Höfer U 2013 Hydrogen diffusion on silicon surfaces *Prog. Surf. Sci.* **88** 61
[26] Khalfaoui N, Rotaru C C, Bouffard S, Jacquet E, Lebius H and Toulemonde M 2003 Study of swift heavy ion tracks on crystalline quartz surfaces *Nucl. Instrum. Methods Phys. Res.* B **209** 165
[27] Schwalb C H, Lawrenz M, Dürr M and Höfer U 2007 Real-space investigation of fast diffusion of hydrogen on Si(001) by a combination of nanosecond laser heating and STM *Phys. Rev.* B **75** 085439

[28] Mette G, Adamkiewicz A, Reutzel M, Koert U, Dürr M and Höfer U 2019 Controlling an S_N2 reaction by electronic and vibrational excitation: tip-induced ether cleavage on Si(001) *Angew. Chem., Int. Ed.* **58** 3417
[29] Skopinski L *et al* 2021 Time-of-flight mass spectrometry of particle emission during irradiation with slow, highly charged ions *Rev. Sci. Instrum.* **92** 023909
[30] Dürr M, Biedermann A, Hu Z, Höfer U and Heinz T F 2002 Probing high-barrier pathways of surface reactions by scanning tunneling microscopy *Science* **296** 1838
[31] Dürr M and Höfer U 2004 Molecular beam investigation of hydrogen dissociation on Si(001) and Si(111) surfaces *J. Chem. Phys.* **121** 8058
[32] Khalfaoui N, Rotaru C C, Bouffard S, Toulemonde M, Stoquert J P, Haas F, Trautmann C, Jensen J and Dunlop A 2005 Characterization of swift heavy ion tracks in CaF_2 by scanning force and transmission electron microscopy *Nucl. Instrum. Methods Phys. Res.* B **240** 819
[33] Schnohr C S, Kluth P, Giulian R, Llewellyn D J, Byrne A P, Cookson D J and Ridgway M C 2010 Swift-heavy-ion-induced damage formation in III–V binary and ternary semiconductors *Phys. Rev.* B **81** 075201
[34] Meftah A, Costantini J M, Khalfaoui N, Boudjadar S, Stoquert J P, Studer F and Toulemonde M 2005 Experimental determination of track cross-section in $Gd_3Ga_5O_{12}$ and comparison to the inelastic thermal spike model applied to several materials *Nucl. Instrum. Methods Phys. Res.* B **237** 563
[35] Osmani O, Medvedev N, Schleberger M and Rethfeld B 2011 Energy dissipation in dielectrics after swift heavy-ion impact: a hybrid model *Phys. Rev.* B **84** 214105
[36] Wilhelm R A *et al* 2017 Interatomic coulombic decay: the mechanism for rapid deexcitation of hollow atoms *Phys. Rev. Lett.* **119** 103401
[37] Karlusic M, Akcöltekin S, Osmani O, Monnet I, Lebius H, Jaksic M and Schleberger M 2010 Energy threshold for the creation of nanodots on $SrTiO_3$ by swift heavy ions *New J. Phys.* **12** 043009
[38] Karlušić M *et al* 2015 Response of GaN to energetic ion irradiation: conditions for ion track formation *J. Phys. D: Appl. Phys.* **48** 325304